STATISTICS, OPTIMIZATION AND INFORMATION COMPUTING
Stat., Optim. Inf. Comput., Vol. **12**, May 2024, pp 713–726.
Published online in International Academic Press (www.IAPress.org)

Finite Element modeling and convergence analysis of a new Biomimetic Branching Structures

Nadir Rihani[1,*], Iatimad Akhrif[1], Mostapha El Jai[1,2], Lamghari Mohamed[3]

[1]*Euromed Center of Research, Euromed Polytechnic School, Euromed University of Fez, Rte Nationale Fez-Meknes, Fez, Morocco*
[2]*Mechanic, Mechatronic and Command Laboratory, ENSAM-Meknes, Moulay Ismail, University, Meknes, Morocco*
[3]*Morocco Automotive Engineering (ENGIMA), 70, Rue N°7, Lot Tazi & Miloud, 20150, Californie, Casablanca, Morocco*

Abstract Branching structures are gaining popularity in the field of advanced structures and building design; they offer high performance in terms of strength and lightweight design, along with the flexibility and precision enabled by modern processing technologies like Additive Manufacturing. This paper provides a concise overview of a geometric design procedure for a novel ribbed class of structures which was previously developed by the authors as a biomimetic optimal Micro-architected dome. Hereinafter, linear lattice models are suggested to carry out structural calculations using the finite element method (FEM). The objective is to examine discretization thresholding and strain energy convergence criteria. Results show that convergence is reached for numbers of elements per leg, ranging from 2 to 6, depending on the geometrical configuration of the dome being studied. The strain energy balance also exposes the influence of each internal force on the total mechanical response of the structure, pinpointing bending moment and axial force as the main decisive factors. As a perspective, the study will focus on limit state design calculations and Analysis of how the local geometry influences the overall stability and strength of this new design.

Keywords Branching structure, Finite Element Method, Convergence, Strain energy balance.

DOI: 10.19139/soic-2310-5070-1964

1. Introduction

Branching structures, as encountered in nature, particularly trees, are an interesting example of biomimicry in civil engineering. These structures offer a remarkable combination of lightness and high mechanical strength. Inspired by nature, engineers seek to replicate these characteristics to optimize the structural efficiency of buildings and achieve significant material savings. By imitating the ramifications of a tree, branching structures effectively distribute loads and optimize stress resistance. This approach, emphasizing lightness with no strength loss, offers vast potential for the construction of more sustainable buildings, while drawing inspiration from the millions of years of evolution that have shaped nature's perfection.

Several numerical methods are available in the literature for designing such branched structures; The double-element method was invented and implemented by Zhao et al. [1, 2] to simulate the elements of branching systems, and a similar process was adopted by Chen, Z et al. for door-type modular steel scaffolds applications [3]. Also, the length penalization method (PLM) and the ground structure modification method (MGSM) are two techniques that were investigated by Cai, Qi et al. [4] to produce diverse lattice configurations. Fengcheng Liu [5] suggests an improved form optimization technique that considers the sensitivity to structural flaws. The result is a strong

*Correspondence to: Nadir Rihani (Email: n.rihani@ueuromed.org). Euromed Center of Research, Euromed Polytechnic School, Euromed University of Fez, Rte Nationale Fez-Meknes, Fez, Morocco

ISSN 2310-5070 (online) ISSN 2311-004X (print)

construction with a low tolerance to imperfections and improved buckling load capability, similarly to the ”GE-SEZ” structure proposed by EL JAI et al. [19]. These techniques are typically embedded in mechanical optimization loops that make use of genetic optimization algorithms and finite elements method for mechanical computations [2, 6, 7, 8, 9, 10, 11]. Other researchers make use of plant growth modeling algorithms such as the L-system method, invent-ed by Lindenmayer in 1989 [12]. This approach is capable of modeling both plant growth and simple cell evolution, and has also been applied in number of papers to design dendriform-like structures [13, 14, 15, 16]. The ”Grasshopper” environment also enabled numerous designers to create sophisticated branching structures using a parametric design workflow.

The use of additive manufacturing is transforming the design and production of branch-shaped structures. This revolutionary technology enables to push back the limits of geometric complexity and offers a new level of design flexibility. In the context of branched structures, additive manufacturing facilitates the production of complicated, interconnected components that resemble natural elements [8, 16, 17]. This method optimizes lightness and mechanical strength by eliminating unnecessary weight while maintaining structural integrity [18]. On the one hand, additive manufacturing reduces material waste, contributing to material efficiency [16, 18], and on the other hand, optimizing scanning strategies can also reduce the energy cost of manufacturing [20]. By combining parametric design, shape generation algorithms and additive manufacturing, it is possible to push back the boundaries of structural efficiency and create branch-like structures that are lightweight, robust and durable, paving the way for a new era of environmentally-friendly engineering and construction [18].

The Finite Element Method (FEM) is a powerful numerical technique employed in mechanical computations to analyze and simulate complex engineering systems such as branching structures. It is based on the concept of subdividing a complex domain into smaller, finite elements, allowing for approximation of behavior within each element. There are two approaches to discretize lattices and branch structures: using volume finite elements to represent the entire branch volume, or using beam finite elements to represent the average branch fiber. The second strategy helps for minimizing the number of nodes and elements in the structure, as well as the overall problem dimension and the corresponding computation costs. According to Galarreta et al. [22], It is preferable to employ volumetric FE analysis for thick-branched structures with a diameter-to-length ratio greater than 0.1, and recommends the use of finite beam elements otherwise for good results accuracy.

However, the FE results can be inaccurate if the mesh quality is not verified, which can bias the convergence of the model. According to Burkhart et al., 39% of papers using FEM do not validate the convergence of the calculations, and 95% do not evaluate the quality of the mesh used in their models [21]. There are various outputs from FEA that can be evaluated to meet convergence criteria, including dis-placement convergence, stress convergence, and stiffness convergence [22, 23, 24]. For regular lattices, these strategies are effective. However, when dealing with a geometrically non-linear structure, it is more appropriate to utilize potential strain energy as a convergence criterion [21, 25, 26].

The aim of this paper is to briefly present the parameterized design of a family of micro-architected domes (MAD), following a biomimetic approach proposed by Nadir et al. [27]. Next, a finite element method (FEM) calculation model is presented. Due to the lack of mesh quality indicators for beam elements in the literature, convergence of potential strain energy is considered here as a validation criterion for mesh quality; an optimization of computational costs has been carried out based on this criterion. Finally, the obtained minimum members are reported, and the corresponding length-to-dome’s radius ratios are statistically discussed to serve as mesh quality indicators for the MAD structure. Last but not least, the impact of internal forces on the MAD structure’s response is investigated by breaking down the global strain energy and analyzing the contribution of each force.

2. Methods

In this section, the global methods used to study this family of domes are outlined; subsection 2.1 briefly presents the design of the family of structures studied, while subsection 2.2 focuses on the analytical formulation of the family’s mechanical problem. Subsection 2.3 covers the strain energy convergence criteria, and 2.4 explains the numerical calculation steps adopted to solve the problem, as well as the overall data workflow.

2.1. Presentation of the MAD family design

The MAD family of structures investigated in this paper is a family of ribbed domes with dendriform geometry proposed by Nadir et al. [27]; the design principle of these structures was based on a biomimetic approach. The parametric design of these structures is established by first duplicating a tetrapod unit cell end-to-end until a pyramidal skeleton is completely filled. Then, a series of three mappings are applied to the intermediate pyramid to achieve the targeted spherical geometry (see Fig.1); these transformations, formulated analytically by Nadir et al. [27], include biomimetic concepts such as the decreasing series of the golden ratio. The macroscale parameters of the MAD structure are the outer radius of the dome R_{ext}, the number of levels n, which governs the density of legs in the structure, and the number of quarters q in the dome, that determine the azimuth angular decomposition (see Fig.2).

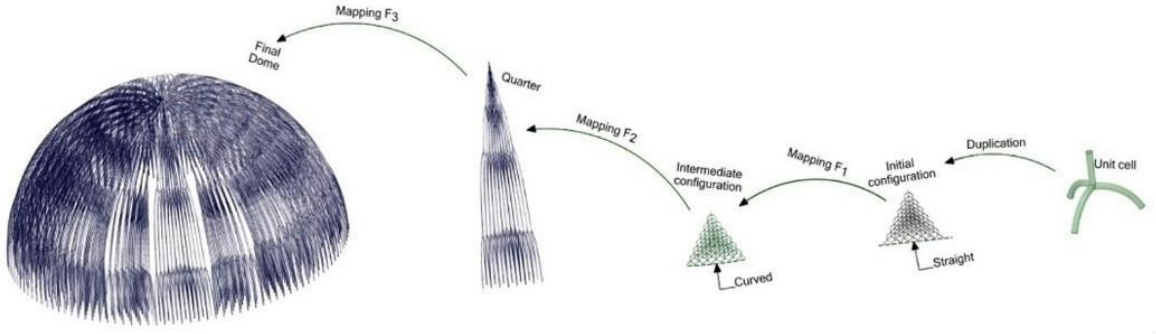

Figure 1. MAD design steps [27]

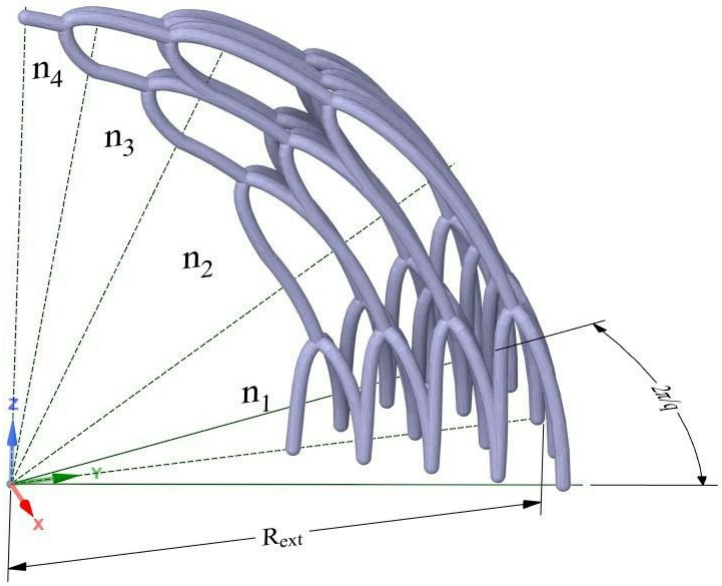

Figure 2. Parametrization of MAD quarter.

2.2. Formal analysis

This section is dedicated to the problem formulation; it includes a brief introduction to elastic beam theory regarding continuum mechanics in terms of constitutive models and potential strain energy formulation.

Theory of elasticity as Mathematical formal framework

The theory of elasticity is a fundamental discipline in continuum mechanics, playing an essential role in understanding the behavior of materials under the influence of external solicitations; when a solid is subjected to deformation, an internal state of stress results, aiming at ensuring the cohesion of the material. The governing equations of the theory are based on fundamental principles of mass conservation and equilibrium reflecting Newton's second law in equation (1). Strain tensor ϵ is expressed in equation (2) as a function of displacement field u. This theory is based on the assumption that most materials can be recovered to their original state once the forces that deformed them are removed, as long as the strains do not exceed a specified state limit. The stresses σ are related to the strains by a linear relationship (3) also known as Hooke's law [28].

$$\nabla.\sigma + f = \rho\ddot{u} \tag{1}$$

$$\epsilon = \frac{1}{2}[\nabla.u + (\nabla.u)^t] \tag{2}$$

$$\sigma = C : \epsilon \tag{3}$$

Where:

- ∇ is the differential operator;
- σ the Cauchy stress tensor;
- ϵ the strain-tensor;
- f the body force per unit volume;
- C the elasticity matrix of the material;
- ρ the material density;

Note that $\rho\ddot{u}$ is negligible for static equilibrium problem.

Beam theory

In beam theory, internal forces are determined by means of the cohesion torsor; the 3D components of this torsor expressed in the beam's local reference frame are : The normal force F_x, the shear force in the y direction F_y, the shear force in the z direction F_z, the bending moment in the y direction M_y, the bending moment in the z direction M_z and the torque M_x (see Fig. 3). In the case of an Euler Bernoulli's beam of length L and cross-section A, the internal forces can be expressed according to the Cauchy tensor σ as indicated in systems (4 and5) [29].

$$\begin{cases} F_x &= \int_A \sigma_{xx} dA \\ F_y &= \int_A \sigma_{xy} dA \\ F_z &= \int_A \sigma_{xz} dA \end{cases} \tag{4}$$

$$\begin{cases} M_x &= \int_A (\sigma_{xz} y - \sigma_{xy} z) dA \\ M_y &= \int_A \sigma_{xx} z dA \\ M_z &= -\int_A \sigma_{xx} y dA \end{cases} \tag{5}$$

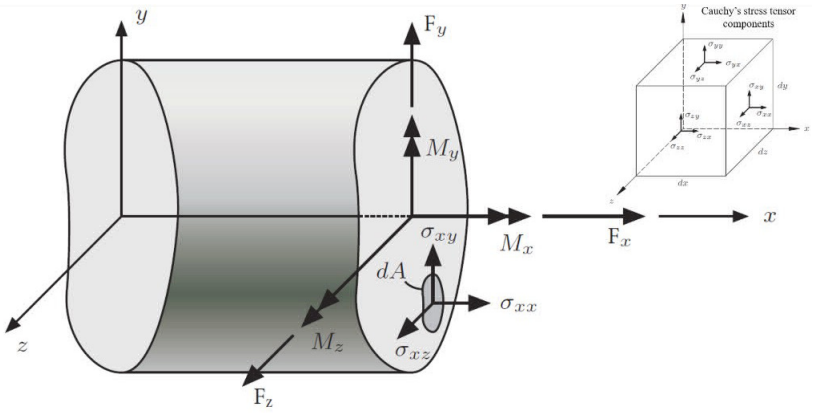

Figure 3. MAD design steps [27]

It is worth mentioning that under elastic conditions, the governing equations for strain and stress in beams can be analogous to those used in elasticity, showing that beam theory can be seen as a simplification of elasticity theory for specific situations. In fact, the internal forces are defined in a beam at each cross-section, unlike the Cauchy tensor, which is defined at every single point of the solid being analyzed so that problem's dimensionality can be considerably reduced.

Potential strain energy

Strain energy is an important concept in the mechanics of materials and structures; it represents the amount of energy conserved in a material or structure during solicitation. This energy, expressed in equation 6, is generally associated with the material's ability to resist elastic deformations. In elasticity, this energy is reversible, meaning that it can be liberated when the deformations are released.

$$W_{tot} = \int_V \bar{W} dV \tag{6}$$

$$\bar{W} = \frac{1}{2} \sum_{i,j=1}^{3} \sigma_{ij} \epsilon_{ij}$$

$\bar{W}$ is the potential strain energy per unit volume. The hook's law can be used to replace the Cauchy tensor components σ_{ij} by the corresponding expressions of ϵ_{ij}.

As for beam elements, the total energy W_{tot} is expressed as a function of the separate internal force torsor components described in systems (4 and 5) as indicated in equation (7).

$$W_{tot} = W_{Axial} + W^y_{Shear} + W^z_{Shear} + W^y_{Bend} + W^z_{Bend} + W_{Tor} \tag{7}$$

Where:

- $W_{Axial} = \int_0^L \frac{F_x^2}{2AE} dx$ is the axial (tensile/compression) component of potential strain energy;
- $W^y_{Shear} = \int_0^L \frac{F_y V^2}{2AG} dx$ is the y-shear component of potential strain energy;
- $W^z_{Shear} = \int_0^L \frac{F_z V^2}{2AG} dx$ is the z-shear component of potential strain energy;
- $W^y_{Bend} = \int_0^L \frac{M_y^2}{2EI_y} dx$ is the y-bending component of potential strain energy;
- $W^z_{Bend} = \int_0^L \frac{M_z^2}{2EI_z} dx$ is the z-bending component of potential strain energy;
- $W_{Tor} = \int_0^L \frac{M_x^2}{2GJ} dx$ is the z-bending component of potential strain energy;

In above expressions, A refers to the cross-section's area of the beam member, E to Young's modulus, and G to shear modulus. I_y, I_z respectively designates the quadratic moment of inertia along y and z axis and J the polar momentum depending on the cross-section's shape.

In finite elements analysis (FEA), number of output values such as strain energy, reaction force, and stress, could be employed as a convergence criterion. However, previous research, especially in micro-architected structures field showed that obtaining a convergent result was simple when using the strain energy or the reaction force, but utilizing stress as the criterion made obtaining a convergent solution challenging [21, 25, 26]. As a result, anytime stress is utilized as a convergence condition, the findings of finite element analyses should be carefully examined.

2.3. Energy convergence criteria

In this subsection, a mathematical description of structures' legs discretization N_{bar}^{min} is formulated to ensure both reliable and economical MAD Finite Element computations. The corresponding convergence criteria are established based on a multi-parametric strain energy analysis; the first convergence parameter is the number of integration points of each bar (NIP) for computing the strain energy per bar, while the second parameter is the number of bars composing each leg of the quarter N_{bar} (see Fig. 4). Computation convergence is assessed by determining the relative strain energy errors between two (NIP) and (N_{bar}) increments, as shown in (8) and (9). The number of integration points converges at NIP^{min} when the ϵ_{NIP} error drops below the 1% threshold, and the number of beams reaches convergence when the ϵ_{bar} error is under 3%.

Convergence stability is considered when 5 consecutive N_{bar} errors are tempted to be below 3%, similarly to the iterative schemes outlined in [30]. The mathematical formulation of NIP^{min} and N_{bar}^{min} are represented by expressions 10 and 11; the relative errors ϵ_{NIP} and ϵ_{bar} were expressed following the approach adopted by [31] for the estimation of errors between the corresponding exact solution and the approximated solution.

$$\epsilon_{NIP} = \left| \frac{W_{tot}(N_{bar}, NIP+1) - W_{tot}(N_{bar}, NIP)}{W_{tot}(N_{bar}, NIP)} \right| \tag{8}$$

$$\epsilon_{NIP} = \left| \frac{W_{tot}(N_{bar}+1, NIP) - W_{tot}(N_{bar}, NIP)}{W_{tot}(N_{bar}, NIP)} \right| \tag{9}$$

$$NIP^{min} = argmin(\epsilon_{NIP}) \tag{10}$$

$$N_{bar}^{min} = argmin\{\epsilon_{bar}(NIP^{min})\} \tag{11}$$

Finally, the converged strain energy of the whole structure W_{tot} is analyzed according to the contribution of each member force presented in expression 7.

2.4. Stepwise computing presentation

In this work, the cross-section of the MAD family of beams is assumed to be hollow circular with external diameter d and thickness e; the ratio of beams diameter d to overall macro-scale MAD diameter $2R_{ext}$ is set at 0.5%, and the ratio of thickness e to diameter set at 2The base nodes are fixed, and an axisymmetric boundary condition is considered at the top of the dome, allowing only one quarter to be studied in order to simplify calculations. Horizontal displacements and rotations along x and z directions at the top of the quarter are blocked (see Fig.4). The structure's self-weight is the only load modelled.

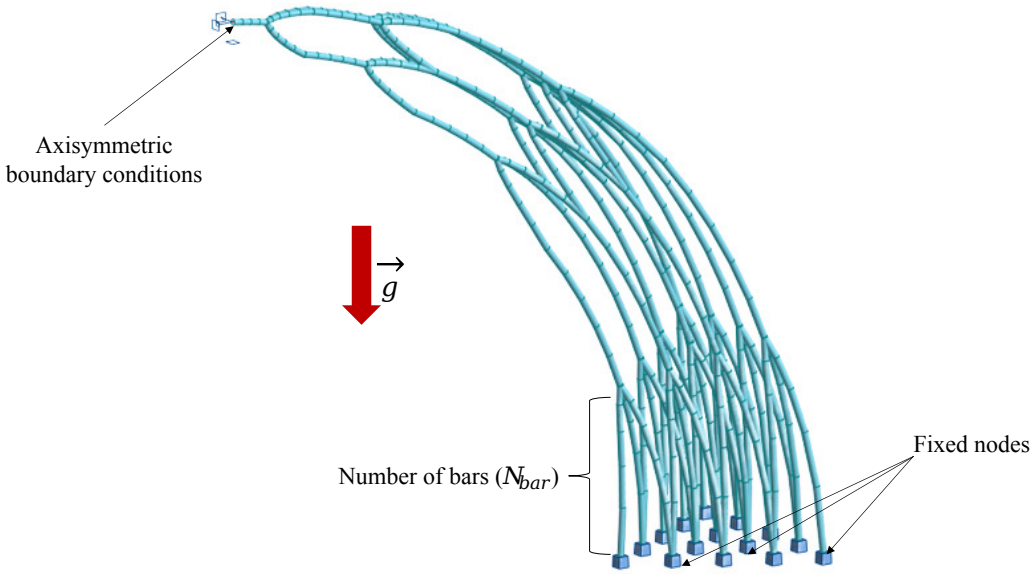

Figure 4. Quarter's finite element model.

The mathematical modeling was implemented using Visual Basic for Application (VBA) in Microsoft environment; Application programming interface (API) allowed connecting the biomimetic method previously scripted on MATLAB [27] to Robot Structural Analysis (RSA) software of Autodesk (see Fig.5). The model's calculations are performed in 7 major steps:

1. Definition of the dome's geometric parameters (R_{ext}, n, q);
2. Initialization of the leg's discretization parameter (N_{bar});
3. Initialization of the number of integration points (NIP);
4. EF model construction and calculation:
   a. Calculation of the nodes and nodal connections of the structure using the successive mapping method proposed in [27];
   b. Definition of loading and boundary conditions;
   c. EF calculation;
   d. Calculation of partial and total strain energies;
5. Calculation of relative errors and verification of convergence criteria according to (NIP) and (N_{bar});
6. Verification of convergence stability;
7. Incremental discretization parameters;

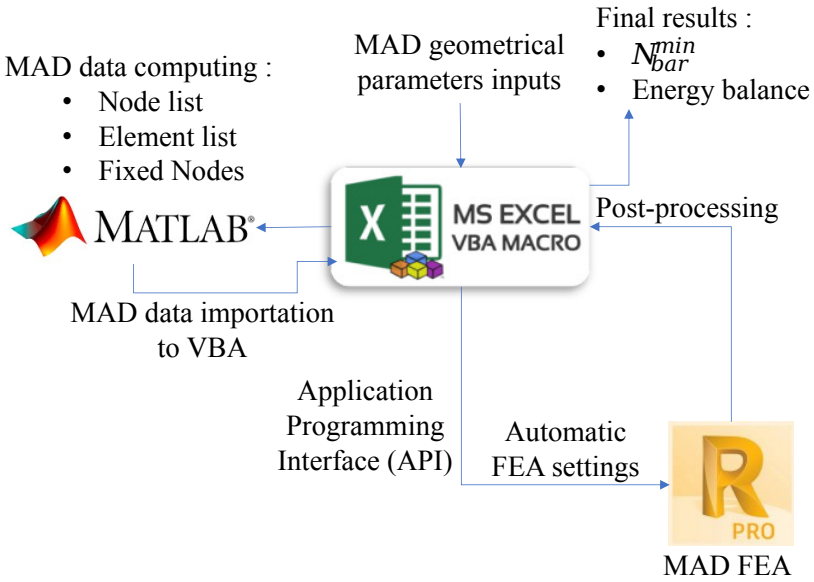

Figure 5. Workflow of the computations.

3. Results and discussion

This section reports the mains findings; the first subsection focuses on the convergence results of the strain energy calculation. Then, the resulting bar lengths are subsequently statistically examined. Finally, the third subsection covers the results on the relative contribution of the different internal forces to the overall strain energy of the structure.

3.1. Convergence analysis of the strain energy

This subsection covers the results from calculation steps in subsection 2.4. The purpose of the computation is to identify the minimum number of bars N_{bar}^{min} in each leg required for convergence of the potential strain energy. As discussed in 2.4, axisymmetric boundary conditions were adopted to reduce problem size and computation cost. For values of n and q ranging from 2 to 9 and 10 to 100 respectively, the response surface representing $N_{bar}^{min}(n, q)$ is plotted (see Fig. 6). It can be observed that the minimal number of discretization of the legs varies between 2 and 6. This parameter is not affected by the quarter parameter q, and instead decreases as the number of levels n increases. In fact, the larger n is, the shorter the legs and the higher their density, which reduces the number of legs required for convergence. Convergence stability was achieved at the first attempt, and the respective errors are less than the 3% threshold (see Fig. 7). Table 1. provides a concise summary of the findings from multiple studies on structural configurations and validation criteria. Galarreta et al. [22] conducted a study on FCC lattices, examining both linear and quadratic configurations, with a particular emphasis on the convergence of stiffness. The first option needed 6 elements per strut, while the second option required 14 elements per strut. In their study, Guo et al. [23] investigated BBC lattices using different parameters (d = 0.5 and d = 0.75). They conducted experimental testing and specified 10 and 20 elements per strut for each parameter, respectively. In their study, Uddin et al. [24] provided valuable insights into a two-layered composite beam. They focused on the importance of displacement convergence and utilized 6 beam elements in their analysis. Compared to the present results, it is noticeable that the optimal number of bars in this model is low compared to literature, since the convergence can be quickly reached when using stain energy as a convergence criterion [21, 25, 26].

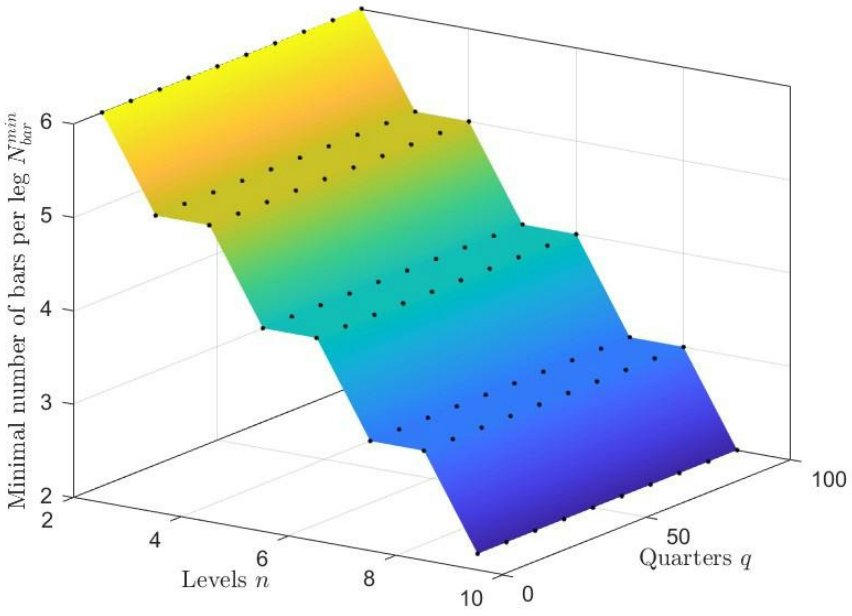

Figure 6. Minimal number of bars needed in each leg for strain energy convergence.

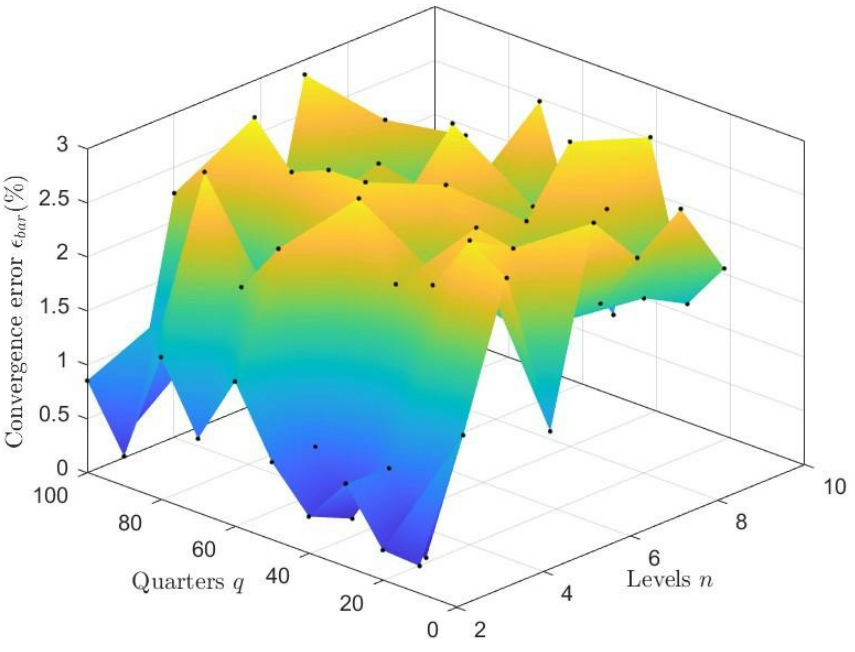

Figure 7. Strain energy error ratio.

Table 1. Literature benchmark on the minimum number of elements for convergence.

Reference	Structure	Validation criteria	Number of elements
Galarreta et al. [22]	FCC lattice (linear)	Stiffness convergence	6 per strut
Galarreta et al. [22]	FCC lattice (Quadratic)	Stiffness convergence	14 per strut
Guo et al. [23]	BBC lattice (d = 0.5)	Experimental testing	10 per strut
Guo et al. [23]	BBC lattice (d = 0.75)	Experimental testing	20 per strut
Uddin et al. [24]	Two-layered composite beam	Displacement conver-gence	6 beam elements
This work	MAD quarter	Strain energy convergence	3 to 6 RSA frame per legs

Regarding the number of integration points, the trapezoidal numerical integration method was adopted. In this case, it was found that the minimum number of integration points NIP^{min} required to reach convergence did not vary with n and q, and was equal to 3 to 4 calculation points per bar since the change of internal forces along the members was low enough. Also, the trapezoidal integration method tends to converge quicker than others. In the following results, integrations are performed through 4 calculation points.

3.2. Bars lengths analysis

The bar lengths of the structures were computed after adopting the minimum discretization already obtained. It turned out that the statistical distribution of these lengths did not follow a conventional distribution. The results revealed that the number of levels n had a much stronger influence on the lengths than the quarter parameter q (see Fig. 8), although some drops in maximum lengths can be observed along the n dimension; this is caused by the transition between one level of discretization N_{bar}^{min} and another. As a result, the maximum length of the bars in each structure varies between 8.5% and 15% of the quarter's overall radius, while the minimum lengths of the bars vary between 0.13% and 2.5% of the quarter's outer radius. The average length value varies between 3.5% and 6.2% of the outer radius, with a standard deviation ranging from 0.04 to 0.0165 (see Fig. 9). These results can be used as maximum length ratio threshold for the FE model in the design of a unique quarter, since they ensure strain energy convergence of FE calculations at less than 3% error.

3.3. Contribution of internal forces to total strain energy

This subsection analyses the contribution of each individual internal force introduced in systems 4 and 5 to the overall strain energy of the structure. This involves understanding the impact of each internal force on the overall mechanical response of the structure. Such analyses are missing from the literature, although they can be an interesting approach for engineers and designers to enhance their understanding of lattice behavior and predict the predominant efforts. Consequently, the analysis focuses on their respective deformation energies in proportion to the overall energy, as well as the evolution of this ratio in (n, q) space (see Fig. 10). Firstly, it is noticed that shear forces and bending moment along the beam's local z axis contribute to less than 5% of the total energy. They are negligible compared to the other components. The contribution of the bending moment along y is the most predominant, reaching 90% of the total energy for almost all structures. Except for high values of n and low values of q, where the contribution of axial energy reaches 40% of the total energy. For low values of q, the torque contribution exceeds 60% of the total energy. This is due to a concentration of torsional moments at the intersections of the legs (see Fig. 11), which are not sufficient because of their large disparity; this concentration is reduced for high values of n, where the number of levels is greater with shorter leg lengths. In order to better investigate the stress concentrations at legs intersections, a 3D XFEM model can be adopted for local induced stress concentrations and crack propagation modeling as it was carried out by Montassir et al. [32].

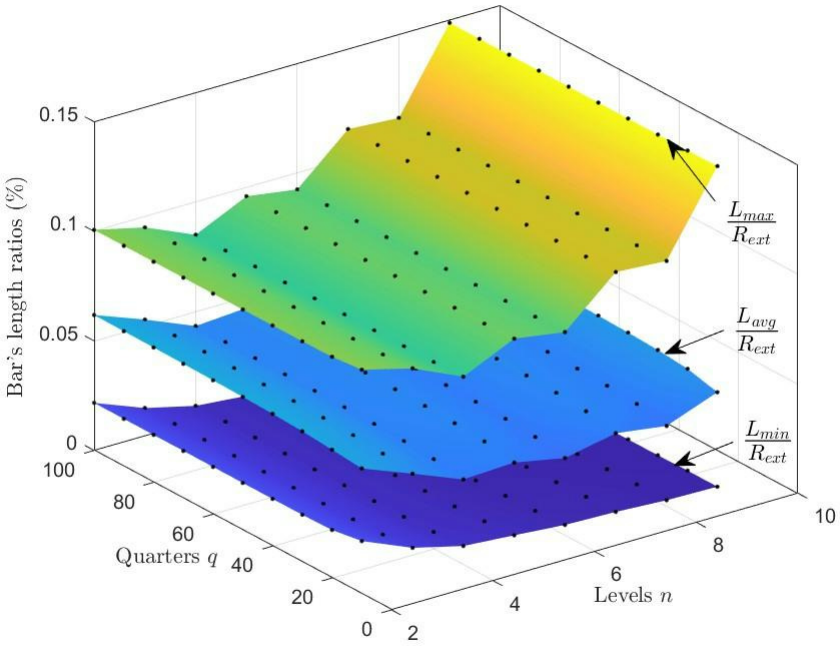

Figure 8. Bar's length ratios vs (n,q).

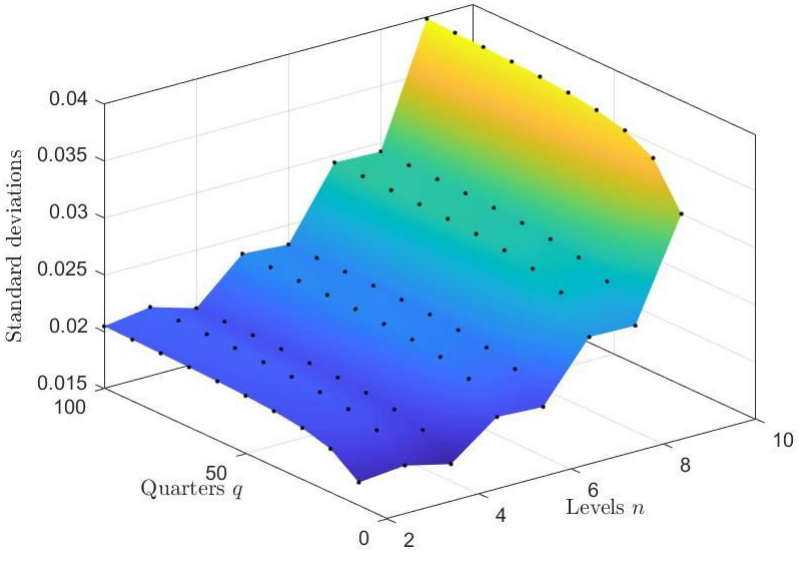

Figure 9. Standard deviations for bar's length ratios.

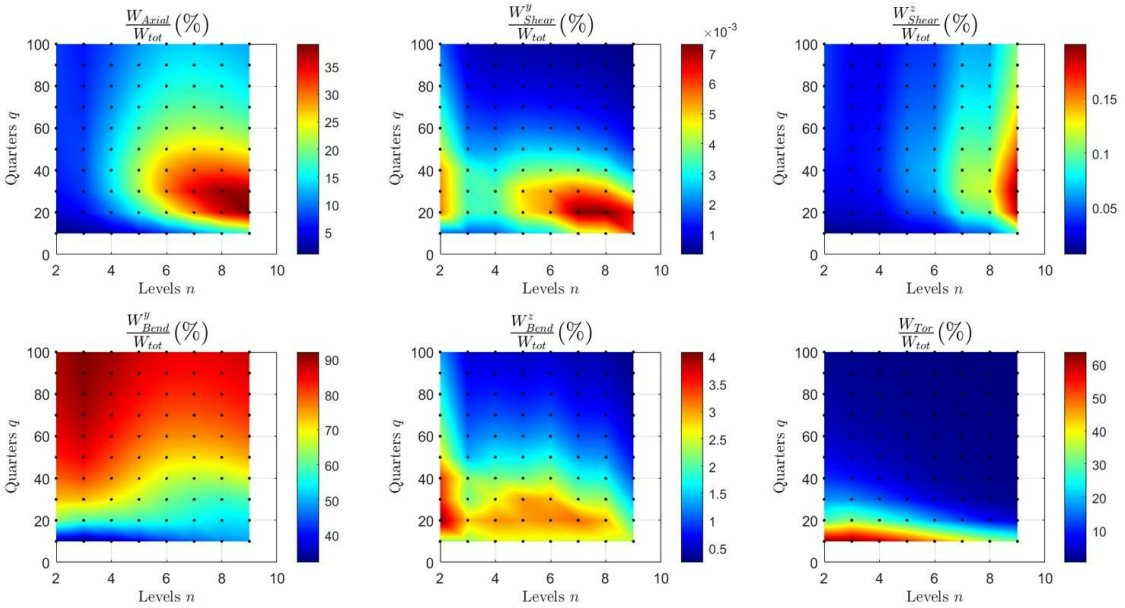

Figure 10. Response surfaces $(n, q, W_i/W_{tot})$ for partial strain energies contributions.

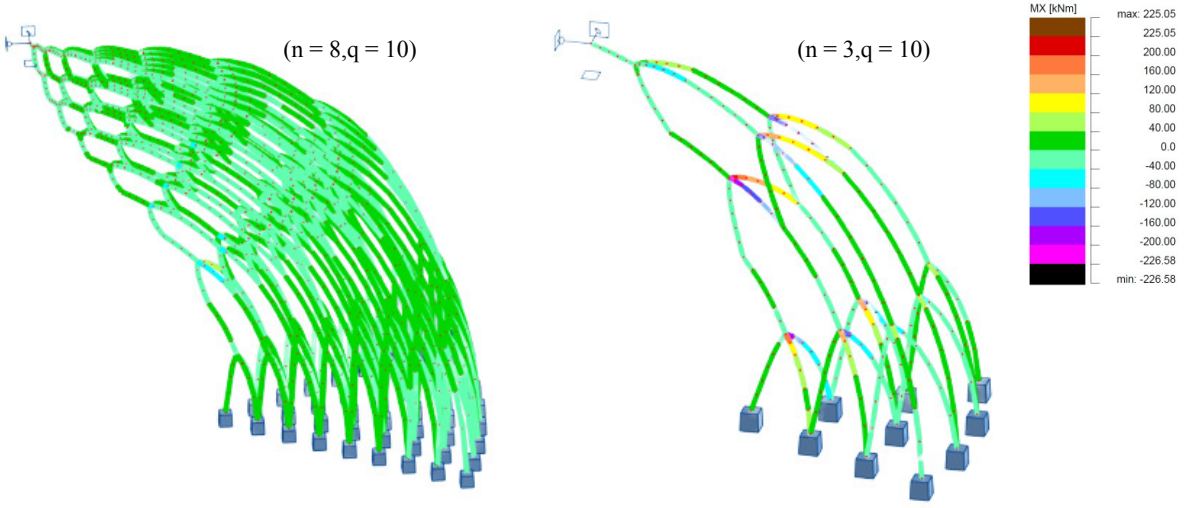

Figure 11. Torque component concentrations in the quarter for high and low n parameter computed.

4. Conclusion and perspectives

In the present paper, a structural analysis is performed on a family of biomimetic branches forming a dome's quarters. Firstly, the analysis focuses on the identification of the minimum threshold for a finite element discretization of the quarter's geometry. This threshold is computed following the convergence criterion of the structure's total strain energy. Its evolution as a function of the quarter's geometrical parameters revealed that branch disparity had no influence on the threshold, and that only branch density varied it. Secondly, the quarter's energy response surface was identified and decomposed according to the 6 internal effort components. One can

therefore detect that the contribution of the axial force and the bending moment is very significant compared to the transverse bending moment and the shear force. Torsion, on meanwhile, might account for a significant contribution in a number of scenarios. Understanding the impact of internal efforts on strain energy is crucial in the field of structural engineering. It helps optimize designs by identifying critical components for refinement, ensuring improved overall performance. Furthermore, this analysis plays a vital role in material selection, offering valuable insights into the behavior of various materials under internal forces and aiding in the decision-making process by considering their mechanical properties. When it comes to additively manufactured structures, which have a natural tendency to be anisotropic and prone to layer sliding, having a deep understanding the strain energy partitioning becomes important. It enables the prediction and prevention of failures, which is essential for designing strong structures that can withstand various types of loads. Further works will focus on Limit States validation for a series of materials and on the effect of d/R_{ext} ratio on the overall stability and resistance of MAD family structures.

Acknowledgement

The authors would like to thank ENGIMA [Website: https://www.engima.ma. Phone: + (212) 5 22 87 91 00] for providing the Robot Structural Analysis software (RSA) which is used to perform FE computations for the present work; many thanks also to Euromed University of Fes for providing Matlab software and Microsoft platform.

Funding

ENGIMA (Morocco Automotive Engineering) company covered the article processing costs (APC).

REFERENCES

1. Zhao, Z., Liang, B., Liu, H., et al. *A novel numerical method for form-finding analysis of branching structures.* J Braz. Soc. Mech. Sci. Eng. 39, 2241–2252 (2017).
2. Zhao Z, Chen Z, Yan X, Xu H, Zhao B. *Simplified numerical method for latticed shells that considers member geometric imperfection and semi-rigid joints.* Advances in Structural Engineering. 2016;19(4):689-702.
3. Chen, Z. & Zhao, Zhongwei. *Analysis of door-type modular steel scaffolds based on a novel numerical method.* Advanced Steel Construction. (2017) 12. 316-327. 10.18057/IJASC.2016.12.3.6
4. Cai, Qi, He, Linwei, Xie, Yi, Feng, Ruoqiang, Ma, Jiaming. *Simple and effective strategies to generate diverse designs for truss structures.* Structures. (2021). 32. 268-278. 10.1016/j.istruc.2021.03.010
5. Liu, F., Feng, R., Tsavdaridis, K. D., Yan, G. *Designing efficient grid structures considering structural imperfection sensitivity.* Engineering Structures. (2020), 204, 109910. doi: 10.1016/j.engstruct.2019.109910
6. Zhao, Z., Liang, B., Liu, H. *Topology establishment, form finding, and mechanical optimization of branching structures.* J Braz. Soc. Mech. Sci. Eng. 40, 539 (2018).
7. Xu, Chao, Wang, Zhengzhong, Li, Baohui, Lau, Daniel. *Form-finding and shape optimization of bio-inspired branching structures based on graphic statics.* Structures. (2021) 29. 392-407. 10.1016/j.istruc.2020.11.028
8. Md Rian, Iasef. *Tree-inspired dendriforms and fractal-like branching structures in architecture: A brief historical overview.* Frontiers of Architectural Research. (2014). 3. 10.1016/j.foar.2014.03.006
9. Von Buelow, Peter. *A Geometric Comparison of Branching Structures in Tension and in Compression versus Minimal Paths.* Conference: International Association of Shell and Spatial Structures (2007).
10. Liu, F., Feng, R., Tsavdaridis, K. D., Yan, G. *Designing efficient grid structures considering structural imperfection sensitivity.* Engineering Structures (2020), 204, 109910. doi: 10.1016/j.engstruct.2019.109910
11. Rodriguez Cabal, M. A., Grisales Noreña, L. F., Ardila Marín, J. G., & Montoya Giraldo, O. D. *Optimal Design of Transmission Shafts: a Continuous Genetic Algorithm Approach.* Statistics, Optimization & Information Computing (2019), 7(4), 802-815.
12. Tuesday, K.C. *An Introduction to Evolution for Computer Scientists. (2008)*
13. Al Khalil, M., Belkebir, H., Lebaal, N., Demoly, F., & Roth, S. *A Biomimetic Design Method for 3D-Printed Lightweight Structures Using L-Systems and Parametric Optimization.* Applied Sciences (2022), 12(11), 5530.
14. Xu, Hua, Wang, Xinyu, Liu, Chia-Nan, Chen, Jiannan, Zhang, Chu. *A 3D root system morphological and mechanical model based on L-Systems and its application to estimate the shear strength of root-soil composites.* Soil and Tillage Research (2021). 212. 10.1016/j.still.2021.105074.
15. Bielefeldt, B. R., Akleman, E., Reich, G. W., Beran, P. S., and Hartl, D. J. (February 22, 2019). *"L-System-Generated Mechanism Topology Optimization Using Graph-Based Interpretation."* ASME. J. Mechanisms Robotics. (2019). 11(2): 020905.

16. Gaudillière-Jami, Nadja, Duballet, Romain, Bouyssou, C., Mallet, A., Roux, Ph, Zakeri, M., Dirrenberger, Justin. *Building Applications Using Lost Form-works Obtained Through Large-Scale Additive Manufacturing of Ultra-High-Performance Concrete.* (2019) DOI: 10.1016/B978-0-12-815481-6.00003-8
17. van Ameijde, Jeroen, Ma, Chun, Goepel, Garvin, Kirsten, Clive, Wong, Jeff. *Data-driven placemaking: Public space canopy design through multi-objective optimisation considering shading, structural and social performance.* Frontiers of Architectural Research. (2021) 11. 10.1016/j.foar.2021.10.007.
18. Du Plessis, Anton, Babafemi, Adewumi John, Paul, Suvash, Panda, Biranchi, Tran, Phuong, Broeckhoven, Chris. *Biomimicry for 3D concrete printing: A review and perspective.* Additive Manufacturing. (2020). 38. 101823. 10.1016/j.addma.2020.101823.
19. El Jai, M., Akhrif, I. & Saidou, N. *Skeleton-based perpendicularly scanning: a new scanning strategy for additive manufacturing, modeling and optimization.* Prog Addit Manuf 6, 781–820 (2021). https://doi.org/10.1007/s40964-021-00197-z
20. El Jai, M., Saidou, N., Zineddine, M. et al. *Mathematical design and preliminary mechanical analysis of the new lattice structure: "GE-SEZ*" structure processed by ABS polymer and FDM technology.* Prog Addit Manuf 6, 93–118 (2021). https://doi.org/10.1007/s40964-020-00148-0
21. Burkhart, Timothy, Andrews, David, Dunning, Cynthia. *Finite element modeling mesh quality, energy balance and validation methods: A review with recommendations associated with the modeling of bone tissue.* Journal of biomechanics. (2013). 46. 10.1016/j.jbiomech.2013.03.022.
22. Ruiz de Galarreta, S., Jeffers, J. R., & Ghouse, S. *A validated finite element analysis procedure for porous structures.* Materials & Design (2020), 189, 108546.
23. Guo, H., Takezawa, A., Honda, M., Kawamura, C., & Kitamura, M. *Finite element simulation of the compressive response of additively manufactured lattice structures with large diameters.* Computational Materials Science, (2020), 175, 109610. https://doi.org/10.1016/j.commatsci.2020.109610
24. Uddin, M. A., Alzara, M. A., Mohammad, N., & Yosri, A. *Convergence studies of finite element model for analysis of steel-concrete composite beam using a higher-order beam theory.* Structures (2020)., 27, 2025–2033. DOI:https://doi.org/10.1016/j.istruc.2020.07.073
25. Berzins, Martin. *Mesh Quality: A Function of Geometry, Error Estimates or Both?.* Engineering with Computers. (1999). 15. 236-247. 10.1007/s003660050019.
26. Sorgente, T., Biasotti, S., Manzini, G., and Spagnuolo, M. *A Survey of Indicators for Mesh Quality Assessment.* Computer Graphics Forum, 42: 461-483. (2023). DOI:https://doi.org/10.1111/cgf.14779
27. Nadir, Rihani, Iatimad, Akhrif, Mostapha, el jai. (2024). *Proposition and Design of a new Micro-Architected Domes family: A Biomimicry-based Approach.* [Accepted Manuscript]. https://doi.org/10.1016/j.foar.2024.01.004
28. Slaughter, W.S. *The Linearized Theory of Elasticity.* Birkhauser, Basel. (2003). https://doi.org/10.1007/978-1-4612-0093-2
29. Lars Andersen and Søren R.K. Nielsen. *Elastic Beams in Three Dimensions.* Aalborg University, Department of Civil Engineering, Structural Mechanics. (2008). DCE Lecture Notes No. 23. Website: https://homes.civil.aau.dk/jc/FemteSemester/Beams3D.pdf
30. Ahmad, I. *Three-step Iterative Algorithm with Error Terms of Convergence and Stability Analysis for New NOMVIP in Ordered Banach Spaces.* Statistics, Optimization & Information Computing, (2021). 10(2), 439-456. https://doi.org/10.19139/soic-2310-5070-990
31. Gazi Karakoc, S. B. *A Quartic Subdomain Finite Element Method for the Modified KdV Equation.* Statistics, Optimization & Information Computing, (2018), 6(4), 609-618. https://doi.org/10.19139/soic.v6i4.485
32. Montassir, Soufiane, Moustabchir, Hassane, El Khalfi, Ahmed. *Application of NURBS in the Fracture Mechanics Framework to Study the Stress Intensity Factor.* Statistics, Optimization & Information Computing. (2023). 11. 106-115. https://doi.org/10.19139/soic-2310-5070-1553